

# RPC-MIP: THE MUTUAL IMPEDANCE PROBE OF THE ROSETTA PLASMA CONSORTIUM

J.G. TROTIGNON<sup>1,\*</sup>, J.L. MICHAU<sup>1</sup>, D. LAGOUTTE<sup>1</sup>, M. CHABASSIÈRE<sup>1</sup>, G. CHALUMEAU<sup>1</sup>, F. COLIN<sup>1</sup>, P.M.E. DÉCRÉAU<sup>1</sup>, J. GEISWILLER<sup>1</sup>, P. GILLE<sup>1</sup>, R. GRARD<sup>2</sup>, T. HACHEMI<sup>1</sup>, M. HAMELIN<sup>3</sup>, A. ERIKSSON<sup>4</sup>, H. LAAKSO<sup>2,5</sup>, J.P. LEBRETON<sup>2</sup>, C. MAZELLE<sup>6</sup>, O. RANDRIAMBOARISON<sup>1</sup>, W. SCHMIDT<sup>5</sup>, A. SMIT<sup>2</sup>, U. TELLJOHANN<sup>2</sup> and P. ZAMORA<sup>1</sup>

<sup>1</sup> *Laboratoire de Physique et Chimie de l'Environnement, CNRS, F-45071 Orléans cedex 2, France*

<sup>2</sup> *Solar System Division, ESA/ESTEC, NL-2200 AG Noordwijk, The Netherlands*

<sup>3</sup> *Centre d'Etudes des Environnements Terrestre et Planétaires, F-94107 Saint-Maur-des-Fossés cedex, France*

<sup>4</sup> *Swedish Institute of Space Physics, S-75591 Uppsala, Sweden*

<sup>5</sup> *Finnish Meteorological Institute, Department of Geophysics, FIN-00101 Helsinki, Finland*

<sup>6</sup> *Centre d'Etude Spatiale des Rayonnements, CNRS, F-31028 Toulouse cedex, France*

(\*Author for correspondence: e-mail: Jean-Gabriel.Trotignon@cnr-orleans.fr)

(Received 2 February 2006; Accepted in final form 28 June 2006)

**Abstract.** The main objective of the Mutual Impedance Probe (MIP), part of the Rosetta Plasma Consortium (RPC), is to measure the electron density and temperature of Comet 67P/Churyumov-Gerasimenko's coma, in particular inside the contact surface. Furthermore, MIP will determine the bulk velocity of the ionised outflowing atmosphere, define the spectral distribution of natural plasma waves, and monitor dust and gas activities around the nucleus. The MIP instrumentation consists of an electronics board for signal processing in the 7 kHz to 3.5 MHz range and a sensor unit of two receiving and two transmitting electrodes mounted on a 1-m long bar. In addition, the Langmuir probe of the RPC/LAP instrument that is at about 4 m from the MIP sensor can be used as a transmitter (in place of the MIP ones) and MIP as a receiver in order to have access to the density and temperature of plasmas at higher Debye lengths than those for which the MIP is originally designed.

**Keywords:** mutual impedance probe, rosetta plasma consortium, rosetta orbiter, thermal plasmas measurements, electron plasma density, temperature, and drift velocity, high-frequency plasma wave measurements, comet dust and gas activity monitoring

## 1. Introduction

*In situ* plasma observations, at about 8,000 km from the nucleus in the tail of Comet 21P/Giacobini-Zinner and at about 15,000 km from Comet 1P/Halley in the sunward direction, yielded electron densities and temperatures of the order of  $10^3 \text{ cm}^{-3}$  and  $10^4 \text{ K}$  in the inner coma when the comets were at heliocentric distances of about 1 AU (Meyer-Vernet *et al.*, 1986; Grard *et al.*, 1989). Such plasma characteristics can be explained in terms of local photoionisation playing a major

role in the ionisation of an outflowing dense atmosphere. Previous missions (ICE, Giotto, Vega 1, Vega 2, Sakigake, Suisei) provided a limited view of the ionised environment around a comet. Rosetta will monitor the comet 67P/Churyumov-Gerasimenko over a longer period of time and from different distances, that should lead to a better understanding of the cometary plasma.

A possible scenario of the evolution of the interaction between 67P/Churyumov-Gerasimenko and the solar wind would be as follows. Beyond 4 AU from the Sun, the solar wind interacts directly with the nucleus whenever the gas production rate  $Q$  is less than  $5 \times 10^{24}$  molecules  $s^{-1}$ . The outflowing atmosphere remains essentially molecular, i.e. collisionless, until about 3.8 AU, where  $Q = 10^{25}$  molecules  $s^{-1}$ . A cometary ionosphere then develops and the mass loading of the solar wind by the cometary ions induces a shock wave. As planned in the Rosetta mission scenario, the Rosetta spacecraft will stay most of the time within a few hundreds km from the nucleus, and will eventually make only some excursions into the inner coma and the plasma tail at distances less than 10,000 km from the nucleus during the Extended Monitoring Phase. Therefore, during this early phase of the comet encounter, Rosetta would always be within the contact surface, a plasma boundary where the inward pressure exerted by the solar wind and its magnetic field is balanced by the outward pressure exerted by cometary gases. The contact surface is the outer edge of a diamagnetic cavity, which contains no magnetic field of solar wind origin since the solar wind cannot penetrate beyond this surface.

The production rate exceeds  $10^{26}$  molecules  $s^{-1}$  within 3.3 AU of the Sun. The effect of collisions becomes more significant and the plasma is in thermal equilibrium with the neutral atmosphere in the inner coma where Rosetta is located. The neutral gas is emitted with a temperature equal to that of the surface of the nucleus (200–300 K), expands with a Mach number of 2–3 and cools adiabatically to 30–100 K within a few cometary radii. The photoelectrons are subject to a strong thermalisation process and their temperature, initially of the order of  $1-2 \times 10^4$  K, eventually reduces to that of the neutral gas. This condition prevails as the comet approaches perihelion and  $Q$  increases towards  $10^{28}$  molecules  $s^{-1}$ .

Wave and particle detectors providing a wide range of measurements are necessary to study the large variety of plasma regimes to be encountered by Rosetta. The Mutual Impedance probe (MIP), as part of the Rosetta Plasma Consortium (RPC), has access to very low electron temperatures (possibly 30 K), which is a great advantage for investigating the ionised constituents of the cometary atmosphere and their interaction with the neutrals. The electron temperature is known to play a major role in physico-chemical processes, in particular the recombination (see for example, Gombosi *et al.*, 1996). MIP will also measure the electron density and the bulk velocity of the ionised atmosphere. In the passive mode, it also has the capability of a plasma wave analyser. In particular, it will detect the spectral distribution of natural plasma waves, in the 7 kHz to 3.5 MHz range, and monitor the dust and gas activities. Table I summarises MIP's expected performance.

TABLE I  
Summary of expected MIP performance.

Quantity	Range
Electron density	2 cm <sup>-3</sup> –1.5 10 <sup>5</sup> cm <sup>-3</sup> ; 5% accuracy 2 cm <sup>-3</sup> –280 cm <sup>-3</sup> for Long Debye Length mode
Electron temperature	30 K–10 <sup>6</sup> K; 10% accuracy
Plasma drift velocity	100 m/s–1,000 m/s; accuracy of about 100 m/s
Frequency domain	7 kHz–3.5 MHz 7 kHz–168 kHz for Long Debye Length mode
Wave: Sensitivity	~ 1 μV m <sup>-1</sup> Hz <sup>-1/2</sup> at 100 kHz
Dynamic range	> 60 dB
Debye length	0.5 cm–20 cm 10 cm–200 cm for Long Debye Length mode
Nominal time resolution	2.5 sec (burst mode) 8 sec (normal mode) 32 sec (survey mode)

The scientific objectives of specific interest to the MIP team are presented in Section 2. MIP's principle of measurements, sensor unit and electronics board are described in Section 3. Section 4 is devoted to the onboard and ground data handling. The distribution of responsibilities among institutes, commissioning measurements, preliminary results of the first Earth swing-by, and the conclusion are given in Sections 5, 6 and 7, respectively.

## 2. Scientific Objectives

MIP's scientific objectives focus on the atmospheric ionisation and thermalisation processes, and the nucleus dust and gas activities. It will fulfil several of the objectives allocated to the Rosetta Plasma Consortium (Trotignon *et al.*, 1999). It will measure the electron density and temperature and, particularly, monitor their variations. It will determine the bulk velocity of the ionised outflowing atmosphere. The investigation of the electron density, temperature and drift velocity will contribute to our understanding of the ionisation, thermalisation and expansion of the cometary atmosphere. As it was mentioned before, the electron temperature is known to be a critical parameter that controls the loss process for the ion population. Measuring the electron temperature down to extremely low values (possibly 30 K) is essential for assessing the efficiency of the plasma-atmosphere interaction and adiabatic expansion in the rapid cooling of the electron population. Observing the variability of these parameters will provide additional insight into the scale length of the gas

jets and lead to possible correlative studies with the results obtained from Rosetta's particle and optical instruments.

MIP's additional goals include defining the spectral distribution of natural plasma waves in the frequency range from 7 kHz to 3.5 MHz, and monitoring the dust and gas activities. Strong plasma waves were observed in the plasma region upstream of 1P/Halley by Vega 1 and Vega 2 (Grard *et al.*, 1987), and in the tail of 21P/Giacobini-Zinner by ICE (Scarf *et al.*, 1986). Nevertheless, no wave measurements were made inside the contact surface, in the close vicinity of the nucleus. If there is very modest cometary outgassing, especially at large heliocentric distances where the solar wind interacts directly with the nucleus, plasma instabilities will develop even if the gas flow is small. Plasma-wave emissions are a very sensitive indicator of outgassing activity. For instance, Shuttle experiments (Gurnett *et al.*, 1988) revealed that significant broadband electrostatic emissions were merely due to small gas releases (leaks, outgassing tiles, thruster firings, water dump). Dust particles impacting spacecraft structures and electric antennas generate electrostatic impulsive signals that can be detected with an electric-field experiment (Gurnett *et al.*, 1986; Trotignon *et al.*, 1987; Laakso *et al.*, 1989; Oberc, 1993). MIP will characterise the spectral distribution of the natural waves and sense the impacts of dust particles. This instrument will therefore explore the nucleus dust and gas activities. It will observe the jets (Trotignon *et al.*, 1991), monitor their onset, follow their development and analyse their spatial and temporal variations as functions of distance from the nucleus and distance from the sun.

### 3. Instrument Description

MIP is a space-qualified instrument for measuring the density, temperature and drift velocity of thermal plasmas. It has proved its efficiency aboard rockets and spacecraft (Chassériaux *et al.*, 1972; Décréau *et al.*, 1978; Béghin *et al.*, 1982). It is particularly suited to the investigation of the plasma environment that will be encountered by Rosetta in the vicinity of the nucleus. MIP's performance relies entirely on the capacitive coupling of two antennas, which do not require any direct contact with the ambient medium. It is thus totally independent of the chemical composition and photoemissive properties of its electrodes and is completely immune, in particular, to contamination by dust and ice deposits. The measurements are not affected by a lack of uniformity of the surface potential. The plasma temperature can therefore be measured down to any arbitrarily value, an asset of paramount importance in a cometary environment where temperatures lower than 100 K are expected.

The MIP is optimized for the inner coma investigations and is designed in such a way that the measuring capabilities match the corresponding objectives. The limits of the frequency range are thus directly related to the extreme plasma density values expected there. The intensity of the injected current is limited by

considerations about the electron temperature and the spacing between the receiving and transmitting electrodes, which determines the size of the sensor, depends upon the ambient Debye length range. The MIP capabilities are summarized in Table 1.

### 3.1. PRINCIPLE OF MEASUREMENTS

An alternating current,  $I$ , with a frequency lying in the range that contains the plasma frequency resonance, is driven through a transmitting electrode. The induced difference in voltage,  $V$ , measured on open circuit between two receiving electrodes is fed into a high-input impedance amplifier. The mutual impedance,  $Z$ , which is then computed onboard, is equal to the ratio of  $V$  to  $I$ . As  $Z$  depends essentially on the properties of the surrounding plasma, the frequency response of the mutual impedance probe may be used for plasma diagnosis. Owing to the resistive, capacitive, and/or inductive nature of the plasma, the frequency response has both real and imaginary components that provide valuable insights into the plasma characteristics.

Figure 1 shows the modulus of the mutual impedance normalised to the vacuum value recorded on ARCAD-3 at the altitude of about 945 km above the Earth's magnetic equator, on 11 March 1982, as a function of frequency (Béghin *et al.*, 1982). The measurements made with the two identical probes mounted head-to-foot are displayed as solid and dashed lines. The two panels correspond to two opposite plasma flow directions; this is discussed further later. Each plot exhibits a peak at

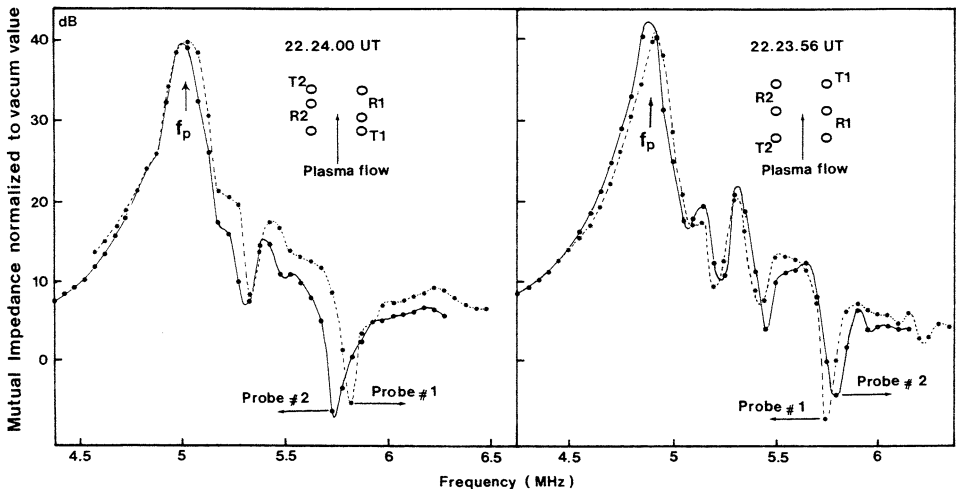


Figure 1. Frequency responses of the two mutual impedance probes that were head-to-foot mounted onboard ARCAD-3. When the magnetic field becomes negligible, the modulus of the mutual impedance exhibits a resonance at the plasma frequency and the interference pattern associated with the electron acoustic wave is shifted in frequency due to a relative plasma velocity around the Earth (from Béghin *et al.*, 1982).

the electron plasma frequency,  $f_p$ , and an interference pattern at higher frequencies, whenever the magnetic field is weak enough to be neglected. Conversely, when the electron cyclotron frequency  $f_{ce}$  becomes of the same order of magnitude as the electron plasma frequency  $f_p$ , other resonances and anti-resonances are usually observed at harmonics of  $f_{ce}$ , the upper hybrid frequency  $f_{uh}$  ( $f_{uh}^2 = f_p^2 + f_{ce}^2$ ), and Bernstein frequencies  $f_{qn}$  (an example is shown in Section 6).

The identification of the single-resonance peak yields the plasma frequency whenever the magnetic field becomes negligible and thus, provides a direct measurement of the electron density,  $n_e$ , via the simple equation  $n_e = (f_p/8.98)^2$ , where  $n_e$  is in  $\text{cm}^{-3}$  and  $f_p$  in kHz. Note that  $f_p$  is also seen in the  $Z$  phase as a sharp variation, so both modulus and phase give accurate  $f_p$  determinations. The amplitude of the resonance peak and the frequency locations of the anti-resonances observed between  $f_p$  and approximately  $1.5 f_p$  gives the Debye length,  $\lambda_D = 6.9 (T_e/n_e)^{1/2}$  (where  $\lambda_D$  is expressed in cm,  $T_e$  in K and  $n_e$  in  $\text{cm}^{-3}$ ) from which the electron temperature  $T_e$  can be derived (Chasseriaux *et al.*, 1972). The interference structure above  $f_p$  is affected by a Doppler shift that is proportional to the projection of the drift velocity along the axis of the sensor (Michel, 1976). This effect is best seen by comparing the measurements obtained alternatively with two symmetric arrangements of the electrode array with respect to the plasma flow. This phenomenon has been observed experimentally in laboratory (Lebreton and Henry, 1980) and in space (Béghin *et al.*, 1982) as illustrated in Figure 1.

To deduce information about the plasma parameters such as  $n_e$  and  $T_e$ , from measurements of  $Z$  at various frequencies, we have to calculate  $Z$  theoretically (Rooy *et al.*, 1972; Béghin, 1995; Geiswiler *et al.*, 2001a,b). The geometry of the device and the influence of the spacecraft, the solar panels included, must be taken into consideration. The former plays a major role when  $\lambda_D$  is of the same order of magnitude as the antenna length, and the latter prevails when  $\lambda_D$  is not small enough when compared with spacecraft structures. Owing to its principle, the mutual impedance technique also implies that the shortest distance between the receiving and transmitting electrodes is greater than about  $2 \lambda_D$ . This distance being 40 cm for the MIP, only plasmas with  $\lambda_D < 20$  cm will be properly analysed by MIP alone (Short Debye Length mode, SDL). In order to overshoot this limit, the Long Debye Length (LDL) mode is implemented on Rosetta. In this mode, the Langmuir probe of the LAP instrument that is about 4 m from the MIP receiver will be used as a transmitter, thus allowing plasmas with  $\lambda_D$  lying in the 20 cm to 2 m range to be investigated. Numerical modellings of both MIP alone and LDL modes are being developed at the Laboratoire de Physique et Chimie de l'Environnement, LPCE. They are based on the Surface Charge Distribution method, which has been used successfully to model the frequency response of electric antennas aboard spacecraft and rockets (Béghin and Kolesnikova, 1998; Kolesnikova and Béghin, 1998). Figure 2 shows the MIP frequency response calculated by taking into account the spacecraft influence (solid line) and neglecting this effect (dashed line). The  $f_p$  resonance peak is sharper and stronger in the former case and anti-resonances are

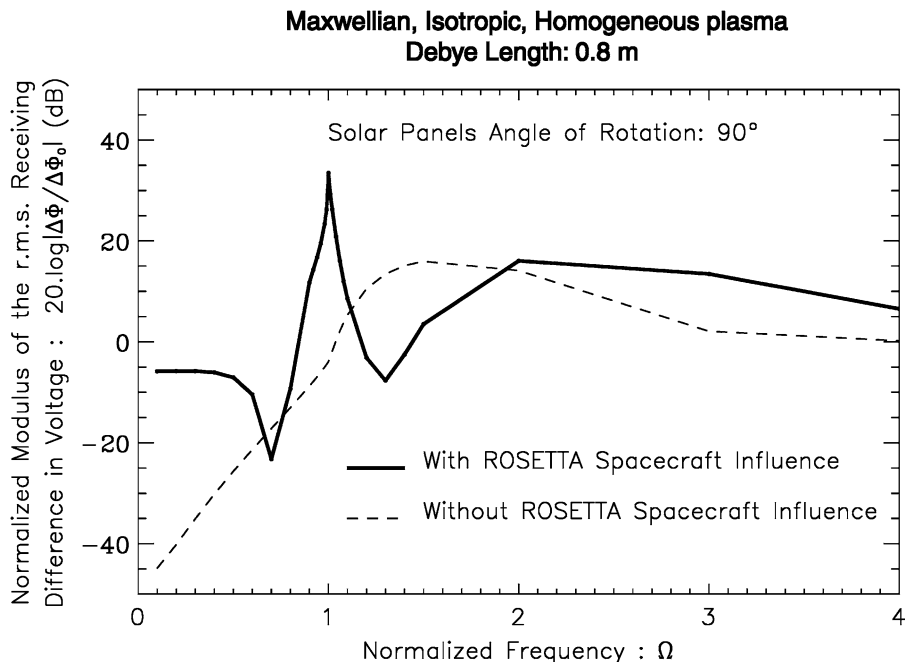


Figure 2. Modelling of the mutual impedance frequency response in the Long Debye Length mode. The spacecraft structures (solid line) modify the frequency response expected in a free space (dashed line).

observed. This result is of the highest importance, for it indicates that  $f_p$  will be measured with improved accuracy and  $T_e$  will also be determined.

In the passive mode, when no current is injected through the transmitting electrode, the sensor is actually a receiving electric antenna. It detects natural waves, and impulsive signals from the expanding plasma clouds generated by dust particles impacting the antenna and the spacecraft, providing that the impact velocity is high enough (Grün, 1981). Wave levels of the order of  $25 \mu\text{V m}^{-1} \text{Hz}^{-1/2}$  were observed at about 8,000 km from 1P/Halley's nucleus in the 0–200 kHz frequency range (Trotignon *et al.*, 1989). By analogy with the measurements performed at an encounter velocity close to  $80 \text{ km s}^{-1}$  near Halley, it is estimated that only particles with dimensions larger than  $10 \mu\text{m}$  can be detected by MIP.

### 3.2. MIP SENSOR

Figures 3 and 4 show the arrangement of the MIP sensor. The electrode array is linear and includes one receiving dipole (R1–R2) and two transmitting monopoles (T1, T2) supported by a Carbon Fibre-Reinforced Plastic (CFRP) cylindrical bar, 103.5 cm in length and 2 cm in diameter. The separation between each receiving

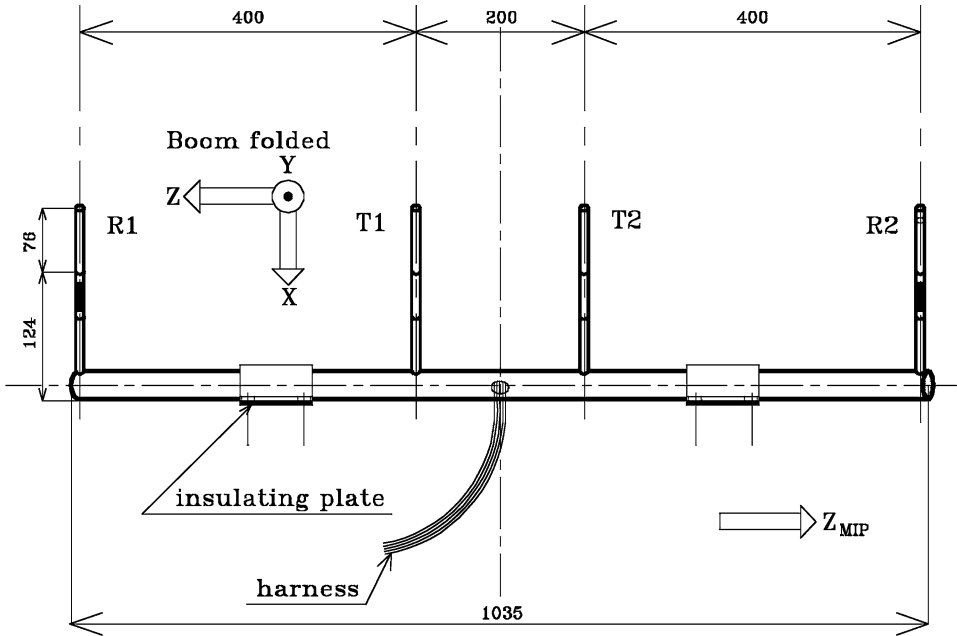


Figure 3. MIP sensor mechanical layout. Lengths are given in mm.

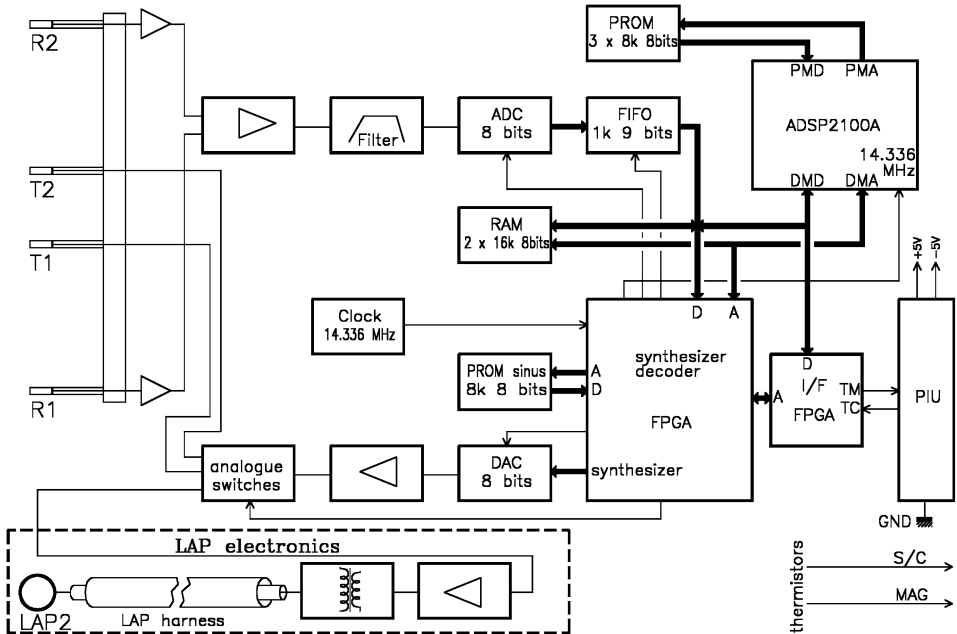


Figure 4. The Mutual Impedance Probe (MIP) block diagram. The MIP electronics board is mainly composed of a Digital Signal Processor (DSP), two FPGAs, an Analogue-to-Digital Converter (ADC), and memories. The MIP sensor and the LAP electronics dedicated to the MIP-LAP Long Debye Length (LDL) mode are respectively shown in the top and bottom left-hand corners.

electrode and the nearest transmitting monopole is 40 cm, in order to measure Debye lengths up to 20 cm. The receiving electrodes are at the ends of the bar in order to maximise the effective length of the antenna for wave measurements, in the passive mode. Each electrode is made of a small metallic cylinder, 1 cm in diameter, mounted at the tip of a CFRP stud, and is electrically uncoupled from this stud by an insulating sheath. The whole CFRP structure is biased to a reference voltage to allow charges to be well distributed: the bar acts as a mirror by producing electrostatic images of the transmitting electrodes.

In active modes, the transmitter injects into the surrounding plasma a current delivered with a very high output impedance. The transmitted signal is composed of 286  $\mu\text{s}$ -long sinusoidal pulses sent every 8 ms, with a magnitude of  $70 \text{ mV}_{\text{rms}}$ . The signal frequency increases from 28 kHz to 3,472 kHz per successively 7, 14, 28, 56, and 112 kHz steps during the Survey mode. In the Long Debye Length mode, the Langmuir Probe sphere that is 4 m from the MIP sensor is used as a transmitter. In this mode the magnitude of the transmitted signal is  $30 \text{ V}_{\text{rms}}$  and the frequencies increase from 7 kHz to 168 kHz in 7 kHz steps. The voltages measured with the receiving electrodes are caught through a very small capacitor (0.12 pF) and amplified by a very high input impedance circuit, located inside the  $R_1$  and  $R_2$  studs. Then they are transmitted, through the harness, to the MIP electronics board. The preamplifier gain is 3 and its sensitivity, referenced to one electrode, is  $0.2 \mu\text{V} \cdot \text{Hz}^{-1/2}$  at 100 kHz.

### 3.3. MIP ELECTRONICS BOARD

The electronics board houses all electronic functions of the instrument. As shown in Figure 4, this board comprises both analogue and digital parts. The analogue part is enclosed in a shield box to reduce the electromagnetic disturbances. The differential amplifier gives  $R_1$ - $R_2$ , an anti-aliasing filter then limits the bandpass to 3,472 kHz. This signal is sampled at 7,168 kHz with an 8-bit resolution Analogue-to-Digital Converter (ACD). The digital part is managed by a Digital Signal Processor (DSP) with the help of a Field Programmable Gate Array (FPGA). In addition to the control of the experiment, the DSP calculates the complex spectra of the signals. It is clocked at 14,336 kHz and works with a code programme contained in three  $8 \text{ k} \times 8$ -bit deep Programmable Read Only Memories (PROMs). The FPGA contains all the logic circuitry to drive the synthesizer and decode the addresses. The data are transmitted to the Plasma Interface Unit (PIU) through an IEEE 1355 serial interface. This bi-directional protocol is controlled by a dedicated FPGA. The synthesis of the transmitted signal is realised by reading, with different steps, a simple digitised sinusoid contained in a  $8 \text{ k} \times 8$ -bit PROM. A Digital-to-Analogue Converter (DAC), followed by a power amplifier, provides a  $1 \text{ V}_{\text{rms}}$  signal to the MIP transmitters or to the LAP electronics board. The MIP board (Figure 5) is

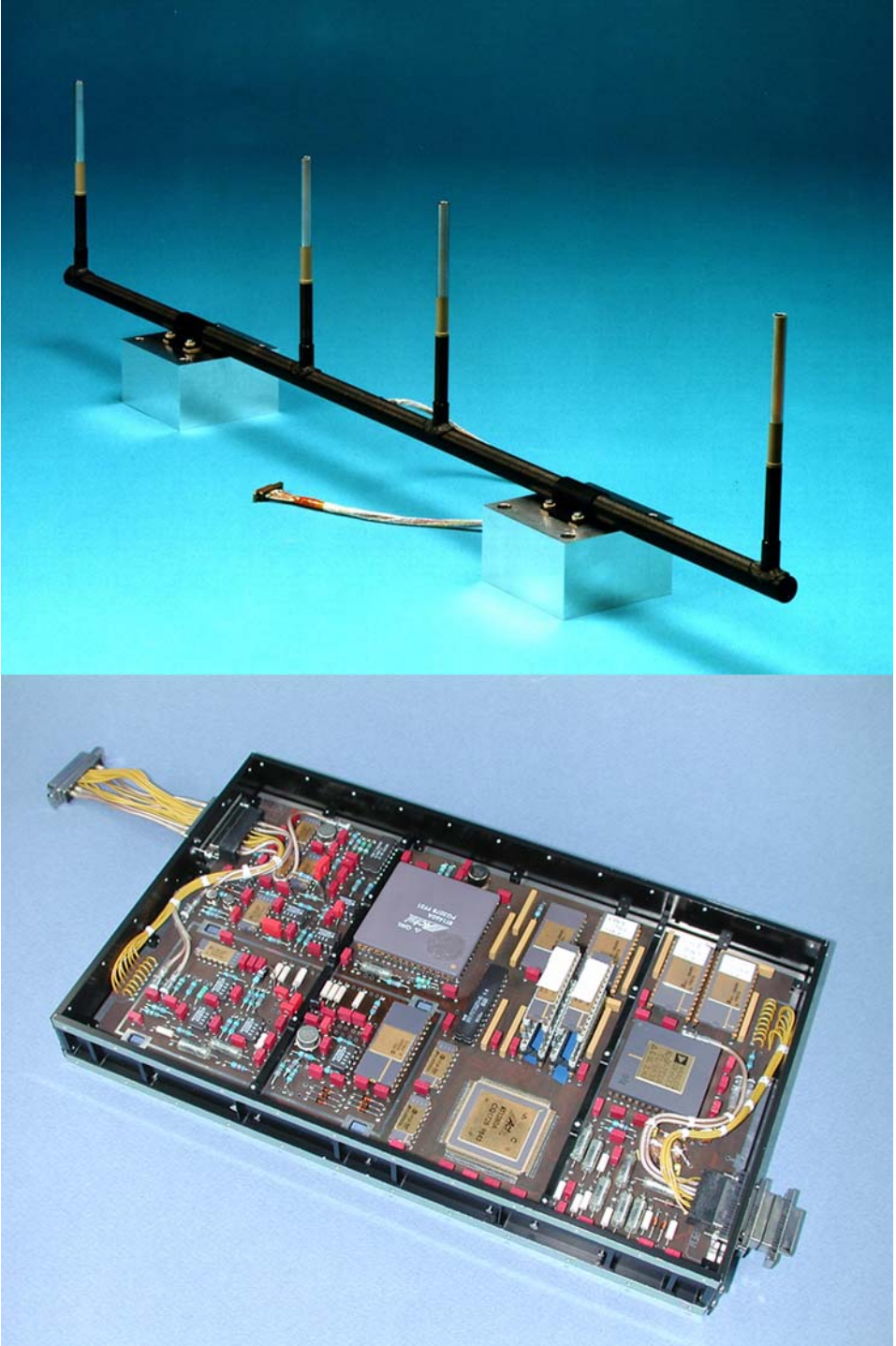


Figure 5. Structural and thermal model of the MIP sensor and flight model of the electronics card.

enclosed in a common box, located on the spacecraft, with the LAP, MAG and PIU electronic boards.

## 4. On-Board and Ground Data Handling

The data received on ground are processed and coded by the onboard software. The original data are then to be retrieved with the help of a decommutation software, used as a component of ground data processing programs such as the ground support equipment, science data processing, and long-term data archiving program packages.

### 4.1. SPECTRUM ANALYSIS

In active modes, when a current is driven through the transmitter, the received signal is windowed and processed onboard with a Fourier analysis. The sampling frequency of the 8-bit ADC is  $f_e = 7,168$  kHz. All the computing tasks are performed by the ADSP 2100 digital signal processor with a clock frequency of 14,336 kHz. A Discrete Fourier Transform is made out of  $N = 1024$  samples, which gives a frequency resolution  $\Delta f = f_e/N = 7$  kHz. When no transmission is applied (passive mode), the antenna measures the natural waves. The samples are processed by a Fast Fourier Transform to yield the power spectrum over the whole frequency range. Again, the maximum frequency resolution is 7 kHz. Only the Fourier component at the emitted frequency is computed and used to construct a full spectrum in the active modes while all the Fourier components are stored to form a natural wave spectrum in the passive mode.

### 4.2. MIP OPERATIONAL MODES

MIP has three different telemetry data rates: 5 (minimum), 50 (normal), and 300 (burst) bits  $s^{-1}$ . The size of a data frame that is transferred to the PIU is fixed and depends on the data rate (18, 198, 1200 bytes, respectively). The acquisition time of a data frame remains constant (32 s). MIP's working modes are organised in 32-s long sequences composed of elementary working modes. These sequences are adapted to the plasma characteristics that will be encountered during the mission. The elementary working modes define how the data to be transferred to the ground, via the PIU, are selected.

### 4.3. MIP GROUND SUPPORT EQUIPMENT

The MIP Electrical Ground Support Equipment (EGSE) is built around a rack-mountable industry PC for stationary use or a labtop-PC for field measurements.

ROSETTA/RPC/MIP – SDL Mode  
2004/05/08 01:46:40

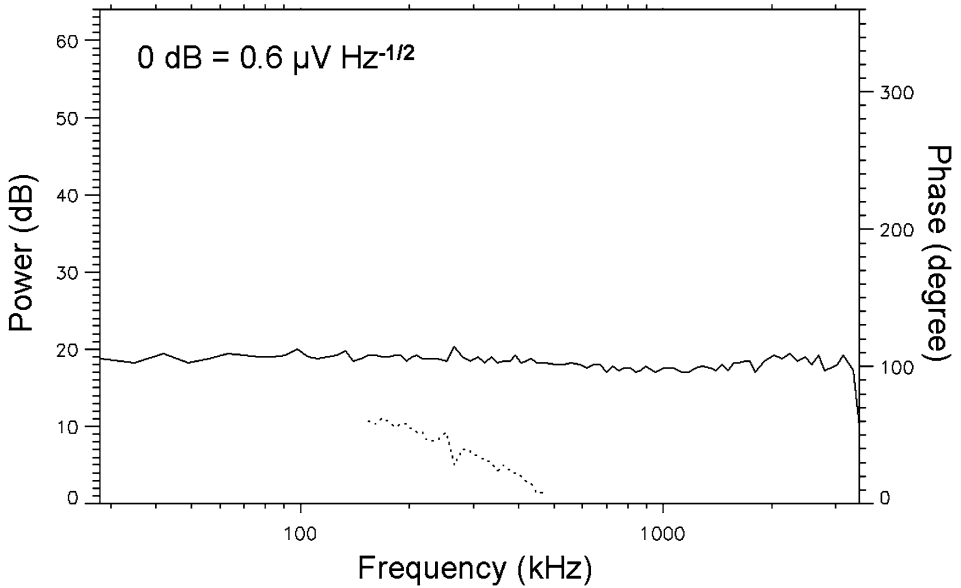


Figure 6. Typical SDL spectrum measured in the solar wind by the MIP instrument onboard ROSETTA during the RPC commissioning phase. The power and phase of the received signal, when 78 mV<sub>rms</sub> were applied on the MIP transmitting electrode, are shown as solid and dotted lines, respectively. Let us note that, in this mode, only the phase measurements made round the frequency at which a maximum in the power is detected are transmitted.

During standalone tests, it is connected to MIP via the PIU-simulator and a serial port. Integrated into the RPC system, the RPC-EGSE interfaces directly to the hardware or the Rosetta ground segment, while the MIP EGSE receives data from it as files via local area network. The EGSE software is based on a Unix operating system (Linux) with ERLANG<sup>TM</sup> as process language, developed by Ericsson, Sweden. The user interface includes graphical display possibilities. Together with its network capability and modular design, it can be adapted easily to changing application needs, monitored via network connection from another location or support given by the EGSE provider in case of questions. Collected data can be written directly to a CDROM as backup. Besides standardised analysis algorithms, additional commercial mathematical software can be used for further processing.

The EGSE's main tasks are data decommutation into physical meaningful parameters, data logging and display. During standalone operation, the EGSE is also able to command all aspects of the MIP instrument and to maintain a record of all command activities.

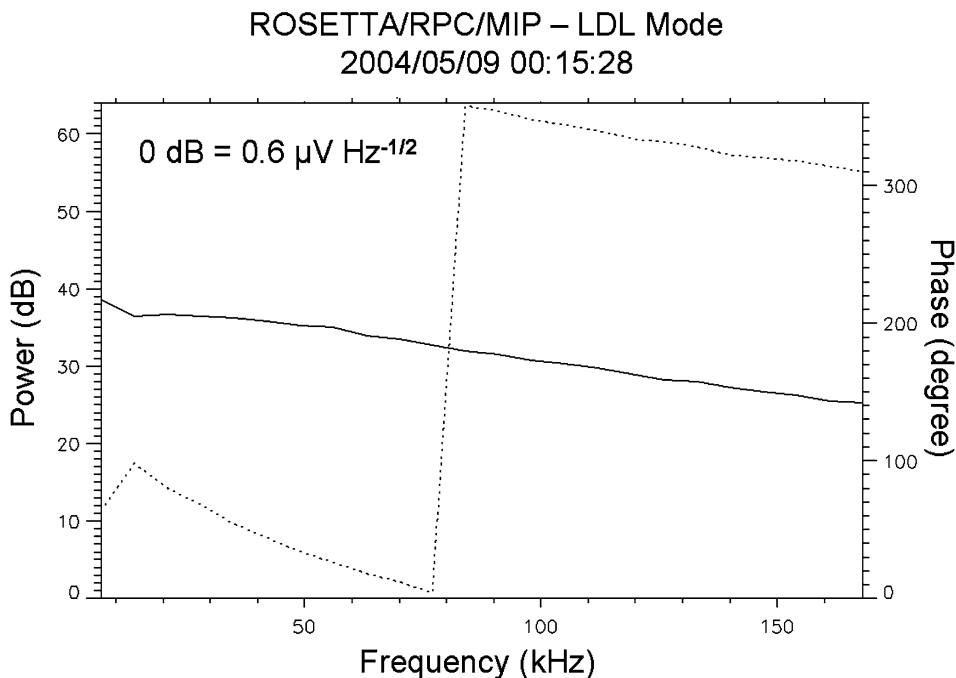


Figure 7. Typical LDL spectrum measured in the solar wind by the MIP instrument onboard ROSETTA during the RPC commissioning phase. The power and phase of the received signal, when 15  $V_{\text{rms}}$  were applied on the LAP transmitting sensor, are shown as solid and dotted lines, respectively.

## 5. Distribution of Responsibilities Among Institutes

MIP's development was shared between three MIP main institutes. The LPCE in Orléans (F) has overall leadership and developed the electronics board. The Solar System Division of the Research and Scientific Support Department at ESA/ESTEC in Noordwijk (NL) is responsible for the design, fabrication and mechanical and thermal testing of the sensor. The EGSE hardware and software is provided by the Finnish Meteorological Institute in Helsinki (FIN). All three institutes are involved in the qualification tests and integration of the MIP to the RPC instrument package. The Swedish Institute of Space Physics in Uppsala (SWE) contributed to the implementation of the Long Debye Length mode. Two other institutes, the Centre d'Etudes des Environnements Terrestre et Planétaires, CETP, in Saint-Maur-des-Fossés (F) and the Centre d'Etude Spatiale des Rayonnements, CESR, in Toulouse (F), provide scientific supports.

## 6. Commissioning and First Earth Swing-by Measurements

The MIP instrument has been declared fully operational after the Rosetta Plasma Consortium commissioning activities, its performances are indeed compliant with

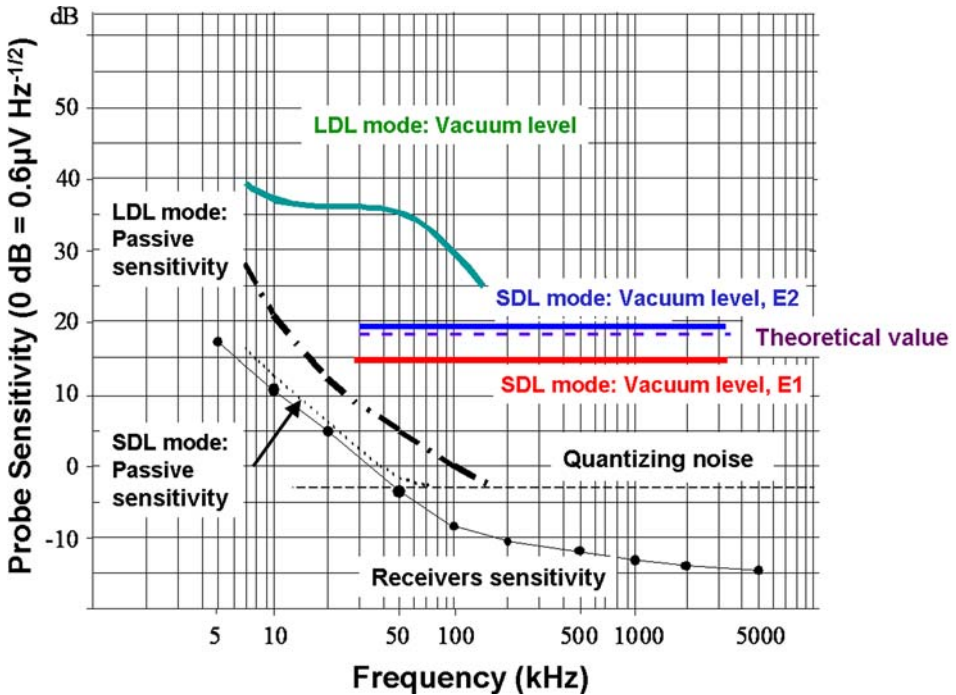


Figure 8. MIP probe sensitivity, in dB above  $0.6 \mu\text{V Hz}^{-1/2}$ , measured during the RPC commissioning phase, in May 2004. E1 and E2 are the two transmitting electrodes of the MIP sensor. Passive and active sensitivity levels are compliant with flight specifications, for both the Short Debye Length (SDL) and Long Debye Length (LDL) modes.

flight specifications. Figures 6 and 7 shows typical spectra recorded during the RPC part 2 commissioning phase, in May 2004, when the MIP SDL and LDL modes were respectively run. The sensitivity levels thus measured are given as a function of frequency in Figure 8. E1 and E2 are the two transmitting electrodes of the MIP sensor.

MIP and the 4 other instruments of RPC were switched on during the first Earth swing-by, in early March 2005. Calibration and general testing were the main objectives, nevertheless valuable observations of the Earth's space environment have actually been made, in particular by the MIP, in the plasmasphere, the cold and high electron-density region dominated by the Earth's magnetic field. One the power spectrum, observed at 2,090-km altitude, is shown in Figure 9. Several plasma resonances and anti-resonances are clearly seen, they are due to the presence of a strong magnetic field. Once identified, the frequency at which they occur gives directly the plasma density and the magnetic field strength: here  $f_p = 1.17 f_{ce} = 468 \text{ kHz}$ , so that the plasma density and magnetic field amplitude are respectively  $2,700 \text{ cm}^{-3}$  and  $14,500 \text{ nT}$ . In addition, the shape of the spectrum gives an estimate

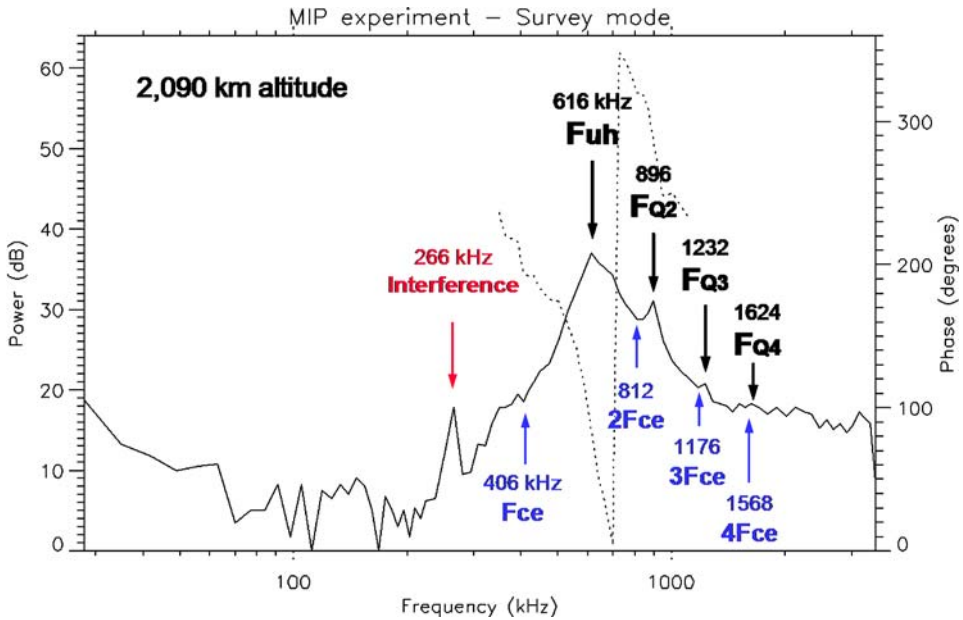


Figure 9. Power spectrum measured in the Earth's plasmasphere at 22:12:39 UT on 4 March 2005 by the Mutual Impedance Probe, MIP, of the Rosetta Plasma Consortium, RPC. Several plasma resonances and anti-resonances are clearly identified. The frequency at which they are observed and the overall shape of the spectrum tell us that the ambient total plasma density, the electron temperature, and the B-field strength are respectively  $2,700 \text{ cm}^{-3}$ , 3,600 K and 14,500 nT.

of the Debye length  $\lambda_D$ , which is a function of the density and temperature. In this case,  $\lambda_D$  is of the order of 8 cm and the electron plasma temperature is therefore of about 3600 K.

## 7. Conclusion

In active mode, the Mutual Impedance Probe, MIP, is particularly suited to measuring the plasma density, electron temperature and plasma drift velocity in cometary environments, and especially the inner coma. Two main modes are possible: for plasma Debye lengths between 20 cm and 2 m, the MIP antenna is used as a receiver and the LAP Langmuir probe which is located in the other boom than the one than supports the MIP sensor may act as a transmitter; conversely, whenever the Debye length is lower than 20 cm, MIP is self-sufficient, its two transmitting electrodes are activated. In passive mode, the MIP will characterize the spectral distribution of the natural waves and monitor the nucleus dust and gas activities of 67P/Churyumov-Gerasimenko. As part of the Rosetta Plasma Consortium, RPC (Trotignon *et al.*, 1999), MIP should contribute to understanding the physico-chemical processes that control the near-nucleus plasma environment as functions of the gas production rate.

## References

- Béghin, C., Karczewski, J.F., Poirier, B., Debrie, R., and Massevitch, N.: 1982, *Ann. Geophysicae* **38**, 615.
- Béghin, C.: 1995, *Radio Sci.* **30**, 307.
- Béghin, C., and Kolesnikova, E.: 1998, *Radio Sci.* **33**, 503.
- Chasseriaux, J.M., Debrie, R., and Renard, C.: 1972, *J. Plasma Phys.* **8**, 231.
- Décréau, P.M.E., Béghin, C., and Parrot, M.: 1978, *Space Sci. Rev.* **22**, 581.
- Geiswiler, J., Béghin, C., Kolesnikova, E., Lagoutte, D., Michau, J. L., and Trotignon, J. G.: 2001a, *Planet. Space Sci.* **49**, 633.
- Geiswiler, J., Trotignon, J.G., Béghin, C., and Kolesnikova, E.: 2001b, *Astrophys. Space Sci.* **277**, 317.
- Gombosi, T.I., De Zeeuw, D.L., Häberli, R.M., and Powell, K.G.: 1996, *J. Geophys. Res.* **101**, 15, 233.
- Grard, R., Scarf, F., Trotignon, J.G., and Mogilevsky, M.: 1987, *Eur. Space Agency Spec. Publ., ESA SP-278*, 97.
- Grard, R., Laakso, H., Pedersen, A., Trotignon, J.G., and Mikhaïlov, Y.: 1989, *Ann. Geophysicae* **7**, 141.
- Grün, E.: 1981, *Eur. Space Agency Spec. Publ., ESA SP-155*, 81.
- Gurnett, D.A., Averkamp, T.F., Scarf, F.L., and Grün, E.: 1986, *Geophys. Res. Lett.* **13**, 291.
- Gurnett, D.A., Kurth, W.S., Steinberg, J.T., and Shawhan, S.D.: 1988, *Geophys. Res. Lett.* **15**, 760.
- Kolesnikova, E., and C. Béghin, C.: 1998, *Radio Sci.* **33**, 491.
- Laakso, H., Grard, R., Pedersen, A., and Schwehm, G.: 1989, *Adv. Space Res.* **9**, 269.
- Lebreton, J.P., and Henry, D.: 1980, *Phys. Letters* **76A**, 49.
- Meyer-Vernet, N., Couturier, P., Hoang, S., Perche, C., and Steinberg, J. L.: 1986, *Geophys. Res. Lett.* **13**, 279.
- Michel, E.: 1976, *J. Plasma Phys.* **15**, 395.
- Oberc, P.: 1993, *Planet. Space Sci.* **41**, 609.
- Rooy, B., Feix, M.R., and Storey, L.R.O.: 1972, *Plasma Phys.* **14**, 275.
- Scarf, F.L., Coroniti, F.V., Kennel, C.F., Gurnett, D.A., Ip, W.H., and Smith, E.J.: 1986, *Sci.* **232**, 377.
- Trotignon, J.G., Béghin, C., Grard, R., Pedersen, A., Formisano, V., Mogilevsky, M., and Mikhaïlov, Y.: 1987, *Astron. Astrophys.* **187**, 83.
- Trotignon, J.G., Grard, R., and Mogilevsky, M.: 1989, *Ann. Geophysicae* **7**, 331.
- Trotignon, J.G., Béghin, C., Grard, R., Pedersen, A., Mogilevsky, M., and Mikhaïlov, Y.: 1991, in A. D. Johnstone (ed.), *Cometary Plasma Processes*, Geophys. Monogr. Ser., vol. 61, AGU, Washington, D.C., p. 179.
- Trotignon, J.G., Boström, R., Burch, J.L., Glassmeier, K.-H., Lundin, R., Norberg, O., Balogh, A., Szegő, K., Musmann, G., Coates, A., Åhlén, L., Carr, C., Eriksson, A., Gibson, W., Kuhnke, F., Lundin, K., Michau, J.L., and Szalai, S.: 1999, *Adv. Space Res.* **24**(9), 1149.